Thermochimica Acta, 199 (1992) 147–157
Elsevier Science Publishers B.V., Amsterdam

A calorimetric approach to the kinetics of the irreversible thermal denaturation of proteins [1]

María L. Galisteo, Francisco Conejero-Lara, Josefa Núñez, Jose M. Sánchez-Ruiz and Pedro L. Mateo

Departamento de Química Física (Facultad de Ciencias) e Instituto de Biotecnología, Universidad de Granada, 18071 Granada (Spain)

(Received in final form 1 August 1991)

Abstract

Differential scanning calorimetry has been used to characterize the thermal denaturation of three proteins: porcine pancreatic carboxypeptidase B, bovine pancreatic α-chymotrypsin and bacteriorhodopsin from the purple membrane of *Halobacterium halobium*. The corresponding thermal transitions were found to be irreversible and rate-limited under some experimental conditions. Kinetic models based on the scan-rate effect on the thermograms have been applied to analyse these irreversible denaturation processes.

INTRODUCTION

High-sensitivity differential scanning calorimetry (DSC) has become one of the most powerful and appropriate techniques for studying protein thermal stability and denaturation, following improvements in its instruments and data analysis, as well as theoretical advances. Indeed, protein folding and stability is currently of particular importance in many aspects of biotechnology. Equilibrium thermodynamic analysis of DSC transitions corresponding to denaturation provides a great deal of information about the energetics and mechanism of the process, and the domain organization and interactions in the protein [1–3]. Clearly, this type of analysis requires chemical equilibrium to be established throughout the temperature range of the transition. Thermal denaturation, however, is often irreversible and rate-limited [4–9]. Analysis of the DSC transitions must then take into account the kinetics of formation of the irreversibly formed protein state. We have recently developed [4–6] some simple kinetic models that appear suitable for the analysis of this type of DSC transition. Klibanov and

Correspondence to: P.L. Mateo, Departamento de Química Física (Facultad de Ciencias) e Instituto de Biotecnología, Universidad de Granada, 18071 Granada, Spain.

[1] Presented at the 12th National Conference on Calorimetry and Thermal Analysis, Bari, Italy, 11–13 December 1990.

co-workers have provided evidence about the nature of the covalent and conformational processes responsible for this irreversible thermo-inactivation of proteins [10–13].

The applicability of this kinetic approach will be illustrated here by the DSC study of three proteins: porcine pancreas carboxypeptidase B (CPB), a zinc exopeptidase, whose thermal denaturation will be shown to follow a very simple kinetic model at different pH values and Zn^{2+} concentrations; bacteriorhodopsin (BR) from the purple membrane of *Halobacterium halobium*, an intrinsic membrane protein with a DSC thermal profile characterized by two endothermic transitions, neither corresponding to a two-state process; and α-chymotrypsin (α-CT), a bovine pancreas endopeptidase that undergoes either reversible or irreversible thermal denaturation, depending on the pH. These three systems represent different situations and raise different questions in the DSC study of their thermal denaturation behaviour.

EXPERIMENTAL

α-CT and di-isopropyl fluorophosphate (DFP)-inhibited α-CT were purchased from Sigma as crystalline powders, stored at $-20°C$, and used without further purification. The CPB was a gift from Dr. F.X. Avilés, and BR was kindly supplied by Dr. E. Padrós. *N*-Acetyl-L-tryptophan ethyl ester and hippuryl-L-arginine, the substrates for the enzymatic assays of α-CT [14] and CPB [15] respectively, were bought from Sigma. All other chemicals used were of the highest purity available; distilled, deionized water was used throughout.

Protein concentrations were spectrophotometrically determined using the molar absorption coefficients 50000 and 63000 M^{-1} cm^{-1} for α-CT [16] and BR [17] at 280 and 568 nm respectively, and an $A^{1\%}_{1\,cm}$ value of 20.0 at 280 nm for CPB [18]. Protein concentrations for DSC experiments were 1.93 mg ml^{-1} for BR, and 1.0–5.0 and 1.7–2.0 mg ml^{-1} for CPB and α-CT, respectively. Concentration ranges of 0.1–1.2 mg ml^{-1} for CPB and 1.6–2.0 mg ml^{-1} for α-CT were used in thermal inactivation measurements.

Thermal inactivation experiments with α-CT and CPB were carried out as described by Galisteo et al. [9] for phosphoglycerate kinase. Briefly, protein samples in closed capillary tubes were placed in a thermostatic bath at a given temperature, extracted at certain times, and cooled immediately in ice prior to measurement of enzyme activity. The decrease of activity with time at each temperature was fitted to a single exponential (first-order kinetics), unless otherwise stated.

Calorimetric experiments were carried out in a computer-interfaced DASM-4 differential adiabatic scanning microcalorimeter designed by Privalov and Potekhin [19,20] with 0.47 ml cells. The scan rates were in the range 0.25–2.0 K min^{-1} and a constant pressure of 2.5 atm was always

maintained. The reversibility of the calorimetric measurements was checked by reheating the sample solution. Instrumental base lines were always subtracted from the experimental endotherms. The resulting difference in heat capacity between the initial (native) and the final (denatured) states was corrected according to Takahashi and Sturtevant [21] to give the temperature dependence of the apparent excess heat capacity of the protein, $C_p^{ex}(T)$. In addition, dynamic correction of the thermograms was carried out as reported by López-Mayorga and Freire [22], using the calculated time constant of the calorimeter. Before the calorimetric experiments, sample solutions were dialysed overnight at 4°C against a large volume of buffer solution with at least one change in the dialysis bath.

DSC thermograms corresponding to irreversible thermal denaturation were analysed according to models based on a kinetic approach for these non-equilibrium processes [4–6].

RESULTS AND DISCUSSION

Carboxypeptidase B

The thermal denaturation of CPB gives rise to a well-defined DSC peak, whose apparent T_m (temperature at the maximum of the heat capacity profile) depends on pH, scan rate and Zn^{2+} concentration. This effect can be seen in Fig. 1, where the thermal denaturation of CPB (C_p^{ex} versus T) at pH 7.5 and 9.0, and at four scan rates is shown. This thermal denaturation was always calorimetrically irreversible. The protein is more stable (higher T_m values) at pH 7.5 than at pH 9.0, while the effect of scan rate on the endotherms clearly indicates that they correspond to irreversible, kinetically controlled transitions. It is thus evident that equilibrium thermodynamics cannot be applied in their analysis.

The thermal denaturation of CPB was analysed with the two-state irreversible model. This is the simplest model for handling DSC non-equilibrium processes under kinetic control [4]. It considers only two significantly populated macroscopic states, the initial or native (N) and the irreversibly arrived at, final or denatured (F) states, i.e. $N \rightarrow F$. Chemical equilibrium between them is not established; the process is characterized by a first-order rate constant k which follows the Arrhenius equation. This model can be shown to be a particular case [4] of that of Lumry and Eyring, $N \leftrightarrows U \rightarrow F$, where U represents the unfolded state of the protein.

Several equations of the model [4] lead to the kinetic parameters of the denaturation process. Thus, k can be obtained from

$$k = vC_p^{ex}/(\Delta H - \langle H \rangle) \quad (1)$$

where v is the scan rate, ΔH the total enthalpy of the transition and $\langle H \rangle$ the excess enthalpy at a given temperature. The activation energy of the

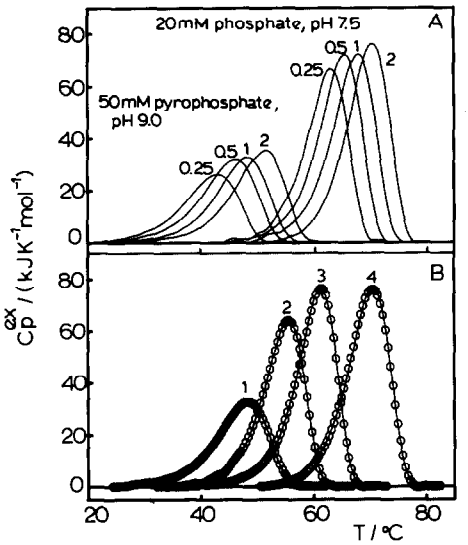

Fig. 1. DSC results for the thermal denaturation of CPB. (A) Temperature dependence of C_p^{ex} for CPB at two different conditions with 1 μm $ZnCl_2$ in both. Numbers correspond to the scan rates used (K min^{-1}). (B) Values of C_p^{ex} for CPB in: curve (1) pH 7.5, 20 mM phosphate, 1 μM $ZnCl_2$, at 2 K min^{-1}; curve (2) pH 9.0, 20 mM pyrophosphate, 1.48 mM $ZnCl_2$, at 1 K min^{-1}; curve (3) pH 9.0, 20 mM pyrophosphate, 0.26 mM $ZnCl_2$, at 0.5 K min^{-1}; curve (4) pH 9.0, 50 mM pyrophosphate, 1 μM $ZnCl_2$, at 1 K min^{-1}. o, Experimental C_p^{ex} data; ———, non-linear least-squares fitting of eqn. (3).

process E can be obtained from an Arrhenius plot of ln k versus $1/T$, as well as from the slope of the plot of $\ln(v/T_m^2)$ versus $1/T_m$ according to

$$\ln(v/T_m^2) = \text{constant} - E/RT_m \qquad (2)$$

Figure 2 shows the linear fitting corresponding to eqns. (1) and (2) for the thermal denaturation of CPB under experimental conditions, including several scan rates, the two pH values 7.5 and 9.0, and two Zn^{2+} concentrations at pH 9.0. The fitting of the calorimetric data to both eqns. (1) and (2) is very good in all cases (Fig. 2). It should be noted that if the CPB denaturation follows the model, the k values calculated by eqn. (1) must be independent of the scan rate, as is the case here (Fig. 2B). In addition, the k values obtained by thermal inactivation experiments for the two Zn^{2+} concentrations at pH 9.0, 20 mM pyrophosphate (Fig. 2B), agree very well with the calorimetric values, and very good fits are again obtained. Furthermore, there was no noticeable effect of protein concentration in the kinetic analysis of both the DSC experiments (1.0–5.0 mg ml^{-1}) and of the thermal inactivation measurements (0.1–1.2 mg ml^{-1}), as expected from the assumption of first-order kinetics in the model.

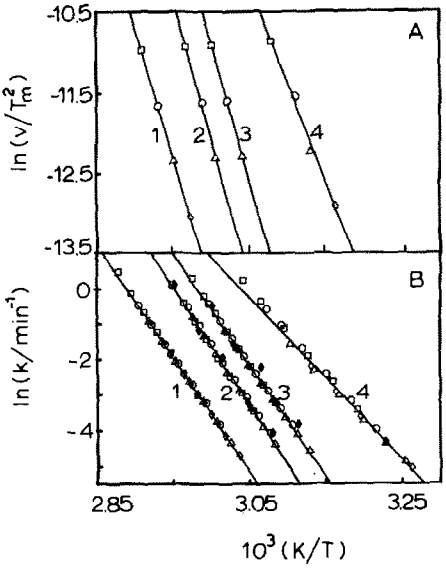

Fig. 2. Plots corresponding to eqns. (1) and (2) for the thermal denaturation of CPB. Numbers 1–4 indicate the same experimental conditions as in Fig. 1B, but here including all the scan rates used. (A) Plot of $\ln(v/T_m^2)$ vs. $1/T_m$: □, 2.0 K min^{-1}; ○, 1.0 K min^{-1}; △, 0.5 K min^{-1}; ◇, 0.25 K min^{-1}. (B) Arrhenius plots: ♦, k values obtained from thermal inactivation experiments; the other symbols have the same meaning as above and correspond to k values calculated from eqn. (1).

The two-state irreversible model predicts quantitatively the temperature dependence of the C_p^{ex} values as given by

$$C_p^{ex} = e\, C_p^m \exp\left[\frac{E(T-T_m)}{RT_m^2}\right] \exp\left[-\exp\left[\frac{E(T-T_m)}{RT_m^2}\right]\right] \quad (3)$$

where C_p^m is the C_p^{ex} value at T_m and e stands for the base of natural logarithms. The excellent fitting of eqn. (3) to the calorimetric data for CPB under some experimental conditions is shown in Fig. 1B.

The activation energy of the denaturation process can be obtained from eqns. (1) – (3), and also calculated directly from yet another equation for the two-state irreversible model [4]

$$E = e\, RT_m^2 C_p^m / \Delta H \quad (4)$$

The E values for CPB given by all four methods agree very well with each other for a given set of experimental conditions. The average E values in kJ mol^{-1} are: 270 ± 4 (pH 7.5, 20 mM sodium phosphate, 1 μM $ZnCl_2$), 270 ± 9 (pH 9.0, 20 mM sodium pyrophosphate, 0.26 mM $ZnCl_2$), 282 ± 6 (pH 9.0, 20 mM pyrophosphate, 1.48 mM $ZnCl_2$) and 196 ± 6 (pH 9.0, 50 mM pyrophosphate, 1 μM $ZnCl_2$). The first three are similar to each other, and to those for the carboxypeptidase A system [7] and thermolysin

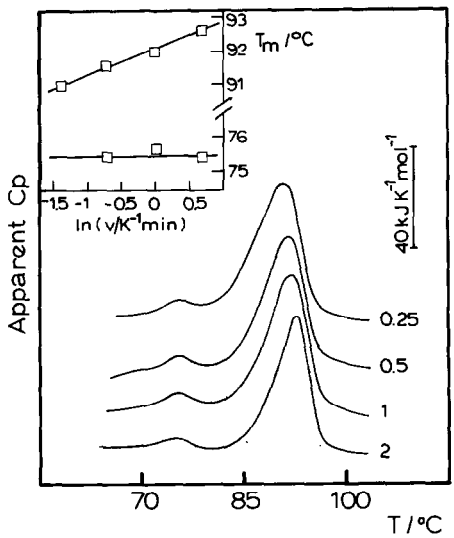

Fig. 3. Calorimetric recordings for the thermal denaturation of BR. DSC thermograms (protein concentration 1.93 mg ml^{-1}) in water after correction for the instrumental base line and the time response of the instrument; the numbers indicate the scan rate used (K min^{-1}). Insert: dependence of the T_m values on scan rate for the two transitions in BR.

[4]. Heavy aggregation was only found in the protein solution after heating, when E dropped to 196 ± 6 kJ mol^{-1}.

The general conclusion of this study is that CPB undergoes a two-state irreversible denaturation process determined by an apparent first-order rate constant that obviously depends on pH and the Zn^{2+} concentration.

Bacteriorhodopsin

The thermal denaturation of BR was studied in distilled, deionized water, pH $\approx$ 6.0, at four scan rates, as shown in the original recordings of Fig. 3. In agreement with the DSC data for the purple membrane [23,24], the denaturation profile shows a small, reversible transition, followed by a higher, irreversible one. We checked the reversible/irreversible character of both transitions as described in the Experimental section. The first transition is ascribed to cooperative disruption of the lattice distribution of BR molecules in the membrane [23], and is not noticably scan-rate-dependent (Fig. 3), as expected from its reversible character. In view of this reversibility, the ratio of the van't Hoff to the calorimetric enthalpy gives an estimate of the average size of the cooperative unit for the transition [25]. This value of about 30 molecules of BR for our system is close to others found for the purple membrane [23,24].

The main, irreversible transition corresponds to the thermal denaturation of the BR molecule [23,24] which is scan-rate-dependent (Fig. 3).

However, it does not follow the predictions of the two-state irreversible model, because different E values are obtained from eqns. (1)–(4); k values calculated by eqn. (1) depend on the scan rate, and there is a poor fitting of eqn. (3) to the experimental C_p^{ex} data. The denaturation mechanism must be more complicated, and could include equilibrium and/or additional irreversible steps and higher order kinetics. We have therefore elaborated a more general model based on the multi-state equilibrium scheme of Freire and Biltonen [26]. Irreversibility is introduced by assuming that any of the equilibrium states (from the native state I_0 to the unfolded one I_n) can undergo a first-order irreversible transition to yield the final state F [5,6]

$$I_0 \overset{K_1}{\leftrightarrows} I_1 \overset{K_2}{\leftrightarrows} I_2 \leftrightarrows \cdots \leftrightarrows I_{n-1} \overset{K_n}{\leftrightarrows} I_n$$

$$I_i \overset{k_i}{\rightarrow} F$$

The mathematical elaboration of the model leads to

$$(\Delta H - \langle H \rangle) = (\Delta H - \langle H \rangle_e) \exp(-F(T)/v) \qquad (5)$$

where ΔH is the enthalpy of the overall denaturation process, $\langle H \rangle$ the excess enthalpy evolved at a given temperature, $F(T)$ a temperature function that includes information about the kinetics of the irreversible steps, i.e. the k_i values, and $\langle H \rangle_e$ an enthalpy average over only the equilibrium states. I_i thus contains the thermodynamic information associated with the DSC transition (in fact, $\langle H \rangle_e$ is the value of $\langle H \rangle$ we would obtain if there were no irreversible processes) [5,6]. Hence, the fitting of

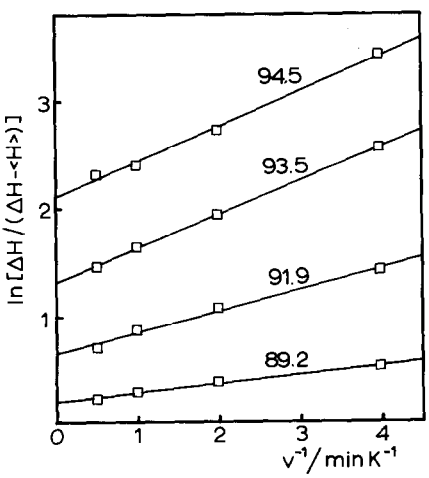

Fig. 4. Plots corresponding to eqn. (5) for the thermal denaturation of BR: □, experimental data corresponding to the four scan rates used at the temperatures (°C) indicated in the figure; ——, linear least-squares fitting of eqn. (5) to the experimental values.

the experimentally attainable $(\Delta H - \langle H \rangle)$ values versus $1/v$ at each temperature leads to both $\langle H \rangle_e$, i.e. information on the equilibrium transitions (which can then be thermodynamically analysed), and $F(T)$, which can provide kinetic information on the possible irreversible processes. A linear least-squares fitting of $\ln[\Delta H/(\Delta H - \langle H \rangle)]$ versus $1/v$ is shown in Fig. 4 to illustrate the thermal denaturation of BR in water at four temperatures for the four scan rates used.

Confirmation of the suitability of this general model to our system and a further analysis of the temperature dependence of $\langle H \rangle_e$ and $F(T)$ (including the proposal of a mechanism for the BR denaturation, its thermodynamic and kinetic parameters and the population of the states involved in the mechanism as a function of temperature) would require additional experiments (effect of concentration, thermal inactivation measurements). We are currently carrying out a more extensive study on this system to propose a general characterization of BR thermal denaturation under different experimental conditions.

α-Chymotrypsin

The fact that the thermal denaturation of many proteins is rate-limited suggests that the operational protein stability may often be determined by the kinetics of irreversible denaturation rather than by the unfolding Gibbs energy, as is usually assumed.

The effect of pH on the DSC transitions for the thermal denaturation of α-CT and DFP-inhibited α-CT provides an example of this kind of situation.

Thermal denaturation of α-CT at pH 2 is fully reversible, as shown by the reproducibility of the DSC transition in the reheating run (Fig. 5A), and closely conforms to the two-state reversible unfolding model, as shown by Privalov and Khechinashvili [27]. Nevertheless, reversibility is heavily dependent on pH. Under our ionic conditions, no reversibility was found at pH ≥ 4 (Fig 5A and 5B). The process responsible for this irreversibility is autolysis of the enzyme, as demonstrated by SDS–PAGE of the samples extracted from the calorimetric cell (results not shown).

The possible rate-limited character of the thermal denaturation of α-CT was investigated by studying the scan-rate effect as measured by the difference (ΔT_m) between T_m at 2 and 0.5 K min^{-1}. The ΔT_m versus pH profile in Fig. 5C shows clearly that the scan-rate effect is strong at pH ≥ 4, indicating that in this pH range denaturation is both calorimetrically irreversible **and** rate-limited. Thermal inactivation experiments (results not shown) also demonstrated that the irreversible process takes place within the temperature range of the DSC transitions obtained at pH ≥ 4. It is interesting to note, nevertheless, that a small scan-rate effect is still observed at pH 2 (reversible denaturation), possibly because at tempera-

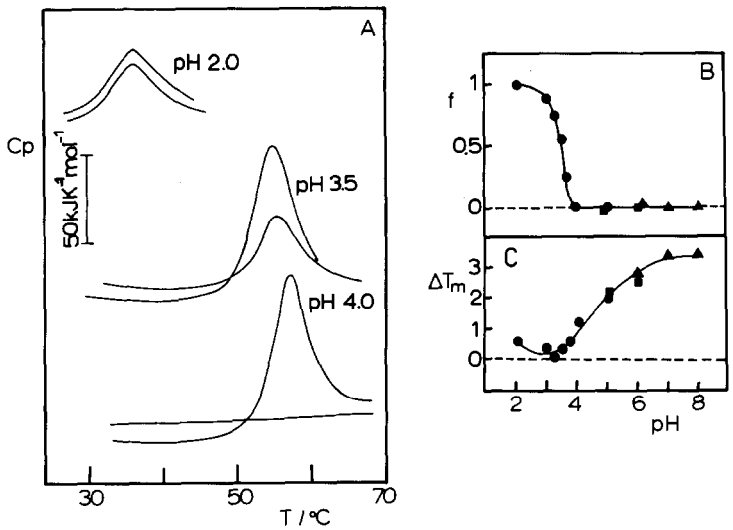

Fig. 5. (A) DSC transitions for the thermal denaturation of α-CT in glycine 50 mM at the indicated pH values. In each case, the first scan (upper transition) and second scan (lower transition) are shown. Note that the first scan was terminated at a temperature slightly above the transition to avoid the effect of irreversible processes that might take place at higher temperatures. (B) Degree of reversibility (f) vs. pH profile for the thermal denaturation of α-CT; f is calculated as the ratio between the excess heat capacities of the maximum for the second and first scans of the same sample (therefore, $f = 0$ when no excess heat capacity was observed in the second scan). The symbols refer to the ionic conditions: ●, 50 mM glycine; ■, 50 mM acetate; ▲, 50 mM phosphate. (C) Scan-rate effect on the DSC transitions for the thermal denaturation of α-CT; ΔT_m = difference between T_m at 2 and 0.5 K min^{-1}. Symbols as in (B).

tures around 36°C (the T_m for the transition at pH 2), the kinetics of folding–refolding is slow (see refs. 5 and 22).

DFP is a covalent α-CT inhibitor that reacts irreversibly with the essential Ser-195. Thus, autolysis of DFP-inhibited α-CT does not appear possible.

DSC of DFP-inhibited α-CT reveals three interesting features: (a) The pH range in which reversibility is found is wider than for active α-CT (Fig. 6A). Nevertheless, no reversibility was observed at pH $\geq$ 5. (b) The main process responsible for irreversibility appears to be aggregation (samples extracted from the calorimetric cell showed strong aggregation in the pH range where irreversibility was found). (c) DFP-inactivated α-CT displays enhanced thermal stability at pH values of around 7.0 (Fig. 6B), where denaturation is irreversible. Its T_m value at pH 8 is, for example, about 8 degrees higher than that for active α-CT under the same scan-rate conditions. It must be noted that only a small difference between the T_m values is observed at pH 2, where denaturation of both proteins is fully reversible (Fig. 6). It appears highly plausible that this enhanced thermal stability at

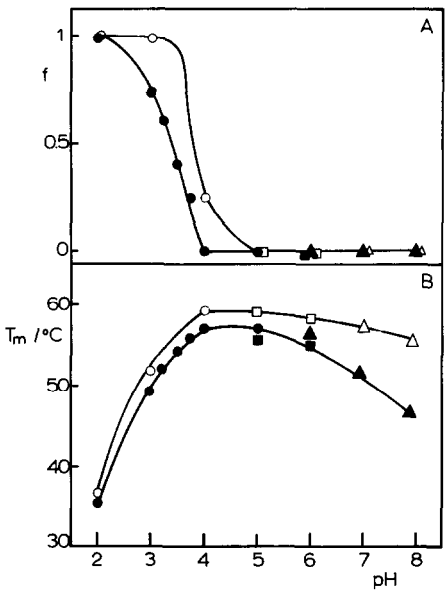

Fig. 6. (A) Degree of reversibility vs. pH profile for α-CT (closed symbols) and DFP-inhibited α-CT (open symbols); f as in Fig. 5. (B) Effect of pH on the T_m values for α-CT (closed symbols) and DFP-inactivated α-CT (open symbols) where the T_m values correspond to 2 K min^{-1}. The symbols refer to the ionic conditions: ●, ○, 50 mM glycine; ■, □, 50 mM acetate; ▲, △, 50 mM phosphate.

neutral pH values stems from the fact that autolysis (the faster irreversible process in this system) is not possible. The kinetics of irreversible denaturation of DFP-inactivated α-CT is thus slower than that of the active enzyme.

The design of new proteins with enhanced thermal stability is an important goal of protein technology. The strategy usually employed consists of introducing changes (mutations, for instance) that are thought to increase the Gibbs energy difference between the native and unfolded states. However, protein thermal denaturation is often found to be irreversible and rate-limited. It appears, therefore, that another valid approach could be to engineer changes that decrease the rate of irreversible denaturation.

ACKNOWLEDGEMENTS

This work was supported by grant PB87-0871 from the CICYT (Ministerio de Educación y Ciencia, Spain) and a grant from Johnson and Johnson. F.C.-L. and J.N. acknowledge PFPI fellowships. We thank Dr. Wayne Bolen for discussion and suggestions on the α-chymotrypsin system.

REFERENCES

1 P.L. Privalov, Adv. Protein Chem., 33 (1979) 167.
2 P.L. Privalov, Adv. Protein Chem., 35 (1982) 1.

3 J.F. Brandts, C.Q. Hu, L. Lin and M.T. Mas, Biochemistry, 28 (1989) 8588.
4 J.M. Sanchez-Ruiz, J.L. Lopez-Lacomba, M. Cortijo and P.L. Mateo, Biochemistry, 27 (1988) 1648.
5 E. Freire, W.W. van Osdol, O.L. Mayorga and J.M. Sanchez-Ruiz, Annu. Rev. Biophys. Biophys. Chem., 19 (1990) 159.
6 J.M. Sanchez-Ruiz, Biophys. J., submitted.
7 J.M. Sanchez-Ruiz, J.M. Lopez-Lacomba, P.L. Mateo, M. Vilanova, M.A. Serra and F.X. Aviles, Eur. J. Biochem., 176 (1988) 225.
8 M. Guzman-Casado, A. Parody-Morreale, P.L. Mateo and J.M. Sanchez-Ruiz, Eur. J. Biochem., 188 (1990) 181.
9 M.L. Galisteo, P.L. Mateo and J.M. Sanchez-Ruiz, Biochemistry, 30 (1991) 2061.
10 S.E. Zale and A.M. Klibanov, Biochemistry, 25 (1986) 5432.
11 D.B. Volkin and A.M. Klibanov, J. Biol. Chem., 262 (1987) 2945.
12 A.M. Klibanov and T.J. Ahern, in D.L. Oxender and C.F. Fox (Eds.), Protein Engineering, Alan R. Liss, New York, 1987, p. 213.
13 D.B. Volkin and A.M. Klibanov, in T.E. Creighton (Ed.), Protein Function: A Practical Approach, IRL Press, Oxford, 1989, p. 1.
14 B. Cerner, R.P.N. Bond and M.L. Sender, J. Am. Chem. Soc., 86 (1964) 3674.
15 J.F. Folk, K.A. Piez, W.R. Carrol and J.A. Gladner, J. Biol. Chem., 235 (1960) 2272.
16 M.A. Marini and C. Wunsch, Biochemistry, 2 (1963) 1454.
17 D. Oesterhelt and B. Hess, Eur. J. Biochem., 37 (1973) 316.
18 F.J. Burgos, Ph.D. Thesis, Autonomous University of Barcelona, 1989.
19 P.L. Privalov, Pure Appl. Chem., 52 (1980) 479.
20 P.L. Privalov and S.A. Potekhin, Methods Enzymol., 131 (1986) 4.
21 K. Takahashi and J.M. Sturtevant, Biochemistry, 20 (1981) 6185.
22 O. López-Mayorga and E. Freire, Biophys. Chem., 87 (1987) 87.
23 M.B. Jackson and J.M. Sturtevant, Biochemistry, 17 (1978) 911.
24 J. Cladera, M.L. Galisteo, M. Duñach, P.L. Mateo and E. Padros, Biochim. Biophys. Acta, 943 (1988) 148.
25 P.L. Mateo, in M.A.V. Ribeiro da Silva (Ed.), Thermochemistry and its Applications to Chemical and Biochemical Systems, Reidel, Dordrecht, 1984, p. 541.
26 E. Freire and R.L. Biltonen, Biopolymers, 17 (1978) 463.
27 P.L. Privalov and N.N. Khechinashvili, J. Mol. Biol., 86 (1974) 665.